Conference Paper, Published Version

Maeno, Shiro; Tomita, Akio

Destruction Prediction of a Rubble Mound Weir Using VOF-DEM Coupled Model

DESTRUCTION PREDICTION OF A RUBBLE MOUND WEIR USING VOF-DEM COUPLED MODEL

Shiro MAENO and Akio TOMITA

[1]Associate Professor, Graduate School of Environmental Science, Okayama University
Tsushima-Naka, Okayama, 700-8530, Japan, e-mail: maeno@cc.okayama-u.ac.jp
[2]Graduate student, Graduate School of Environmental Science, Okayama University
Tsushima-Naka, Okayama, 700-8530, Japan

ABSTRACT

Nature friendly hydraulic structures such as a rubble mound weir have attracted attention in recent years. Therefore, it is important to establish an analytical model to analyze the flow around such a porous weir. The aim of this study is to develop a destruction prediction model for the rubble mound weir under a gradual increase of discharge. The VOF (Volume of Fluid) method was used for the flow analysis around and through the rubble mound weir, and the DEM (Distinct Element Method) was used to express the failure process. A proposed VOF-DEM coupled model can feed back the movement of the DEM particles to the flow analysis of the VOF. It is confirmed that the proposed model can reproduce the step by step destruction of the rubble mound weir similar to the experimental results.

Keywords: nature friendly structure, rubble mound weir, natural stone, VOF, DEM

1. INTRODUCTION

Recently many nature-oriented river works were carried out to restore the river environment. Considering this background, use of a porous weir made of natural stone is expected as an alternative structure of an impermeable weir made of concrete or steel because a porous weir excels in river environment. Michioku et al. (2003, 2004, 2005a, 2005b) investigated a rectangular porous weir experimentally and theoretically. They showed a practical discharge equation for a porous weir. Maeno et al. (2002, 2004, 2005) also clarified the failure process of a trapezoidal weir composed of natural stones experimentally. Maeno et al. (2004, 2005) applied numerical wave flume, which was developed by Isobe et al. (1999, 2001), to the flow over a porous weir. In the basic equation, Maeno et al. introduced the porous resistance term which can express the difference in the permeability of the porous weir, and they clarified its validity. Ito et al. (2002) and Maeno et al. (2005) investigated soil-water-structure interaction using the Distinct Element Method. Failure processes such as a submerged breakwater and a rubble mound weir were shown by their study. However, the coupling method used in the model has a problem. That is, the movement of the DEM particles was not taken into account on the flow analysis. In addition porosity variation due to the movement of DEM particles was not taken into account.

Considering this background, this study aimed to develop a destruction prediction model for a rubble mound weir under a gradual increase of discharge. The VOF (Volume of Fluid) method was used for the flow analysis around and through the rubble mound weir, and the DEM (Distinct Element Method) was used to express the failure process. A proposed VOF-DEM coupled model can feed back the movement of the DEM particles to the flow analysis of the VOF. Numerical results were compared with the experimental results and applicability of the proposed numerical model was evaluated.

2. OUTLINE OF THE ANALYSIS

2.1 Outline of the flow analysis

To simulate the flow over and through a porous weir, the following basic equations were used. In these equations the effects of a porous medium were expressed by using the porosity n, which was introduced by Edward et al. (2000), Michioku et al. (2005c).

$$\frac{\partial u}{\partial x}+\frac{\partial w}{\partial z}=0 \tag{1}$$

$$n\frac{\partial u}{\partial t}+\frac{\partial uu}{\partial x}+\frac{\partial wu}{\partial z}=-n^2\left(\frac{1}{\rho}\frac{\partial p}{\partial x}-g_x-R_x\right)$$
$$+\frac{\partial}{\partial x}\left(n\nu_e\left[2\frac{\partial u}{\partial x}\right]\right)+\frac{\partial}{\partial z}\left(n\nu_e\left[\frac{\partial u}{\partial z}+\frac{\partial w}{\partial x}\right]\right)-\frac{2}{3}\frac{\partial k}{\partial x} \tag{2}$$

$$n\frac{\partial w}{\partial t}+\frac{\partial uw}{\partial x}+\frac{\partial ww}{\partial z}=-n^2\left(\frac{1}{\rho}\frac{\partial p}{\partial z}-g_z-R_z\right)$$
$$+\frac{\partial}{\partial x}\left(n\nu_e\left[\frac{\partial w}{\partial x}+\frac{\partial u}{\partial z}\right]\right)+\frac{\partial}{\partial z}\left(n\nu_e\left[2\frac{\partial w}{\partial z}\right]\right)-\frac{2}{3}\frac{\partial k}{\partial z} \tag{3}$$

$$n\frac{\partial F}{\partial t}+\frac{\partial uF}{\partial x}+\frac{\partial wF}{\partial z}=0 \tag{4}$$

Here, n is the porosity, t is the time, x,z are the space coordinates, horizontal and vertical respectively, u,w are the flow rate components in x and z directions, g_x, g_z are the acceleration components, R_x,R_z are the flow drag components, ρ is the density of fluid, and p is the pressure. The terms to take into account turbulence are as follows: k is the turbulent energy, ε is the turbulent energy dissipation ratio, ν the molecular viscosity coefficient, ν_t is the kinematic eddy viscosity, and $\nu_e=\nu+\nu_t$. Standard $k-\varepsilon$ model was used in this study. With respect to R_x,R_z, the following equations were used. In the equations, not only the laminar effect but also the turbulent effect was considered.

$$R_x=u\left(\frac{\nu}{K}+\frac{C}{\sqrt{K}}\sqrt{u^2+w^2}\right) \tag{5}$$

$$R_z=w\left(\frac{\nu}{K}+\frac{C}{\sqrt{K}}\sqrt{u^2+w^2}\right) \tag{6}$$

$$K=n^3D_{sp}^2/\{k_1(1-n)^2\},\qquad C=k_2/\sqrt{k_1n^3} \tag{7}$$

u,w are the mesh averaged velocities, D_{sp} is the diameter of the particle, (k_1, k_2)=(200, 2.8) were used in this study considering the numerical experiment by Maeno et al. (2007).

2.2 Outline of the DEM

The DEM was used to model the deformation of the porous weir which is collapsed easily under a flood flow (Gotoh and Sakai (1997) and Gotoh et al. (2000)). The interaction between pairs of particles of coordinates (x_i,z_i) is modeled with an elastic spring and the viscous dash pot. Circle shape particles were used in this study. Motion of the particles is caused by the drag force due to seepage flow and pressure gradient. components F_x and F_z calculated by the VOF modules. The governing equations for the DEM particle at (x_i, z_i) can be written as follows:

$$(M_i + M_i')\ddot{x}_i = \sum_j \{-f_n \cos\alpha_{ij} + f_s \sin\alpha_{ij}\}_j + F_x \tag{8}$$

$$(M_i + M_i')\ddot{z}_i = \sum_j \{-f_n \sin\alpha_{ij} + f_s \cos\alpha_{ij}\}_j - (M_i - \rho_w V_i)g + F_z \tag{9}$$

$$I_i\ddot{\theta}_i = \frac{d_i}{2} \cdot \sum_j \{f_s\}_j \tag{10}$$

where the subscripts i, j indicate specific particles, θ_i is angular velocity, f_n, f_s are the normal and tangential forces acting at the contact point of two particles, M_i is the particle mass, a_{ij} the contact angle between contacting particles, V_i is the particle volume, I_i is the momentum of inertia, d_i is grain diameter, ρ_w is the density of the water, M_i' is the added mass. The added mass M_i' is given as $M_i' = \rho C_M V_i$, where the added mass coefficient $C_M = 0.5$ was used. F_x, F_z are the external forces transmitted from the fluid to the DEM particles. In the present research the forces are composed of the drag due to the flow F_D and due to the pressure gradient F_S.

$$F_x = F_{D_x} + F_{Sx}, \quad F_z = F_{D_z} + F_{S_z} \tag{15}$$

The external force due to the drag from flow F_D is calculated using the following expressions:

$$F_{D_x} = \frac{1}{2}\rho C_D A_{pi}\sqrt{(U - u_{pi})^2 + (W - w_{pi})^2} \cdot (U - u_{pi}) \tag{16}$$

$$F_{D_z} = \frac{1}{2}\rho C_D A_{pi}\sqrt{(U - u_{pi})^2 + (W - w_{pi})^2} \cdot (W - w_{pi}) \tag{17}$$

$$C_D = 0.4 + \frac{24\nu}{\sqrt{(U - u_{pi})^2 + (W - w_{pi})^2}\, d_i} \tag{18}$$

where U and W ($U = u/n$, $U = w/n$) are the velocities in x and z directions respectively, u_{pi} and w_{pi} are the instantaneous particle velocities in x and z directions respectively, A_{pi} is the cross-section area of the particle, and C_D is the drag coefficient. The seepage velocities U and W are calculated by the VOF module for centers of cells, therefore in case a particle located by parts in two cells, the average value is taken.
The external force component F_S originates from the water pressure gradient force acting on particle volume V_s. The spring constant and the damping coefficient of the viscous dash pot of the DEM particles are calculated automatically due to the mass of the particle and an incremental time step (see Gotoh and Sakai; 1997 and Gotoh et al.; 2000).

2.3 Numerical model and conditions

(a) Numerical model

Figure 1 shows a rubble mound weir model used in the numerical analysis. This model corresponds to the experimental model used by Maeno et al. (2002). The weir was composed of natural stone and its mean particle size is about 4.8 cm. In the experiment, the rubble mound weir was destroyed at its downstream slope under over flow condition. **Figure 2** shows the numerical mesh used in the VOF analysis and initial packed state for the DEM analysis. The lowest particles are fixed to the bottom and other particles were packed using free packing method due to gravity. Mesh sizes for the VOF analysis are 2.5 cm in the x direction and 1.0 cm in the z direction respectively. The lowest mesh size in the z

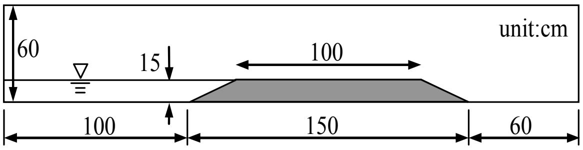

Fig.1 Numerical model

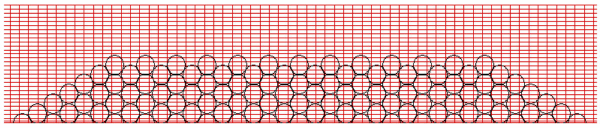

Fig.2 Initial packing and mesh for the VOF analysis

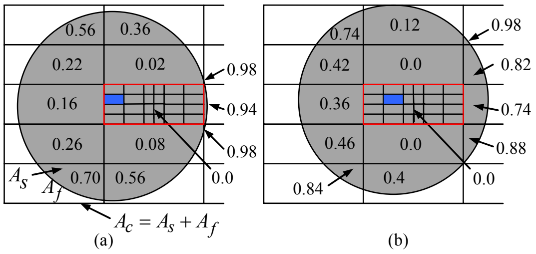

Fig.3 Porosity adjustment

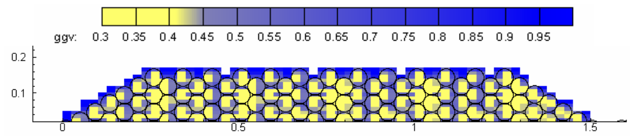

Fig.4 Porosity distribution at initial state

direction is 0.5 cm.

(b) Numerical condition

The discharge condition was set referring to the experimental results by Maeno et al. (2002). In the experiment, the rubble mound weir started to destruct at the quantity of 15 l/s. And the destruction progressed step by step. Therefore the discharge in the numerical analysis was set 10 to 25 l/s, and it was increased linearly taking 120 seconds. Incremental time step Δt was 1.0×10^{-4} (s), added mass coefficient was $C_M = 1.0$, inter-frictional coefficient between particles μ was 0.577 and that between wall and particles was 0.176.

2.4 Coulpling VOF-DEM

In the VOF analysis, as described in Eqs. (2) - (4), the porosity of the porous region must be properly given. And in the DEM analysis, as shown in Eqs. (5) - (7), the porosity also becomes an important factor to calculate the drag force caused by the flow. Significant changes of porosity are expected during a destruction process of the rubble mound weir, and therefore the parameter has to be updated according to movements of the rubble when coupling VOF-DEM analysis. Maeno et al. (2006) proposed the porosity estimation method in the VOF-DEM-FEM coupled model for the submerged breakwater. In their model, the size of the DEM particle was smaller than the numerical grid size. If the DEM particle is larger than the grid size, the model can not be applied (see **Figure 2**). Therefore, in this study the following new method was proposed.

Figure 3 shows the state of the mesh and the DEM particle. The center of the particle is located at the rectangular part filled with blue color. Values in the Figure show the porosity in each cell. In this study, the particle is assumed in a two-dimensional cylindrical shape. Therefore, as shown in **Figure 3 (b)**, if the cell is fully shaded by the DEM particle, the porosity in the cell becomes zero (see the red frame cell in **Figure 3 (b)**).

As described above simple calculation of the void area in the two dimensional domain, based on the arrangement of the DEM cylinders is obviously underestimated compared to a three-dimensional matrix of spheres. In this research, a new effective method is proposed to handle changes of the porosity related to the movement of the DEM particles even in a two-dimensional domain. First, particle area A_s occupied for each cell was calculated. Then the porosity n was rectified using experimentally obtained porosity $n_{\exp} = 0.41$.

$$n = (A_f + A_s n_{\exp})/(A_f + A_s) \tag{11}$$

where, A_f is a rate of porous area except for the particle for each cell. The area of

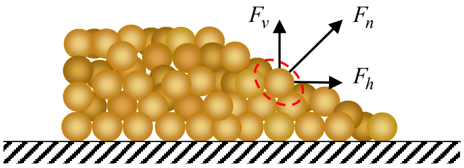

Fig.5 Tensile test

Table 1 Tensile force in each direction

F_v	F_n	F_h
2.81N (287g)	3.04N (311g)	4.75N (485g)

corresponding cell A_c is $A_s + A_f$.

Although the porosity can be calculated using Eq. (11), the calculation load increases when the change of the porosity due to the movement of the particle is calculated in every time step. Therefore the following method was adopted in this study. First, the cell where the center of the particle exists divided into small sub-areas. A_f of the surrounding cells was calculated in advance for every sub-area. For example, Figure. 3 (a) shows values of A_f when the center of the particle is in the blue color sub-area. It is possible to give the porosity only in the decision of the particle location. If there are two particles in the same cell, A_f was superimposed.

Figure 4 shows the porosity distribution in and around the porous weir. As shown in this Figure, the porosity of the porous weir was properly given and the effectiveness of the proposed method was confirmed. Proper value of the porosity can help proper evaluation of the porous resistance in the VOF analysis.

2.5 Outline of the experiment

(a) Experimental results for rubble mound weir

Maeno et al. (2002) showed that initial destruction of the rubble mound weir starts with a removal of a few stones along the downstream slope of the weir. Afterwards, the destruction of the downstream slope progresses gradually. The destruction of the rubble mound weir does not progress continuously; but it progresses with a collapsing stage and a stable stage alternately. Considering the seepage force distribution in the rubble mound weir, Maeno et al. (2002) concluded that not only the tractive force but also the seepage force would be the causing factors in the early stage failure of the downstream slope. And the failure of the weir progresses with an increase of the effect of the tractive force of the overflow.

(b) Tensile force

As shown in **Figure 5**, tensile strength was measured by a pulling test of the stone located on the downstream slope of the weir. In the experiment tensile force to vertical, horizontal and normal direction against the slope were measured using a spring balance. The slope of the weir was 27° with reference to Maeno et al (2002, 2004). Each experiment was performed ten times. **Table 1** shows mean values of the test results. The tensile forces for vertical and normal directions are about 60% of the horizontal force. This result means that the pressure of the normal direction might have a large effect on the removal of the stones on the slope. And this result also supports Maeno el al.'s result that the removal of stones is caused by the pressure gradient.

3. NUMERICAL RESULTS

3.1 Destruction process

In the experiment, an initial destruction started when the discharge reached about

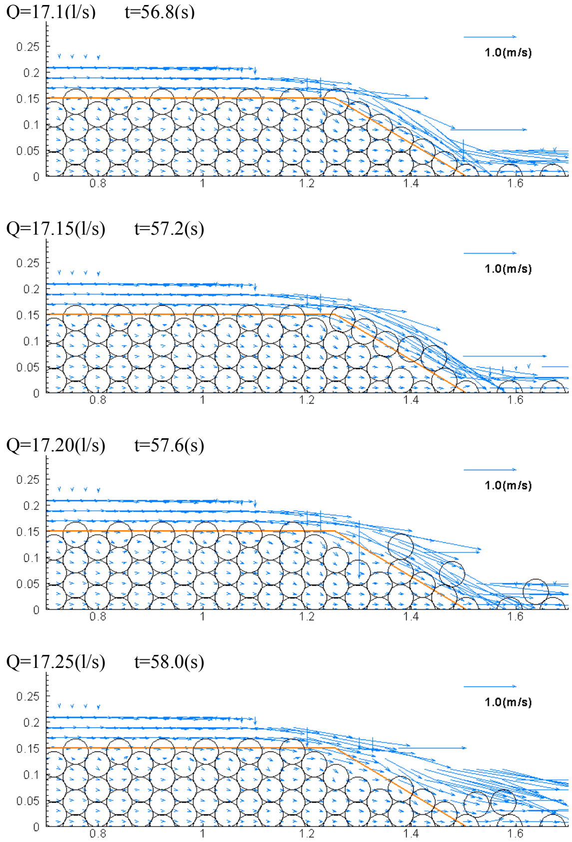

Fig.6 Second stage destruction process and velocity distribution

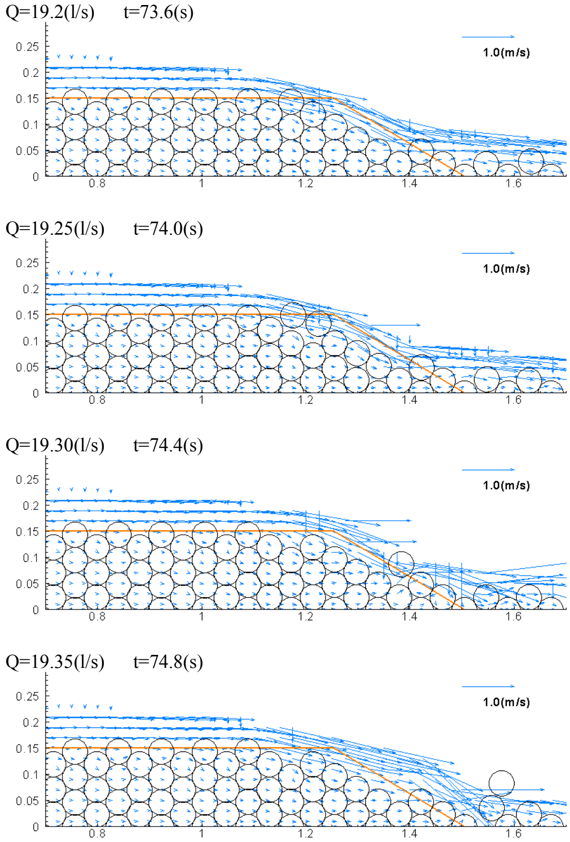

Fig.7 Third stage destruction process and velocity distribution

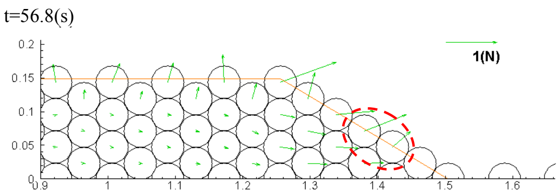

(a) Second stage destruction

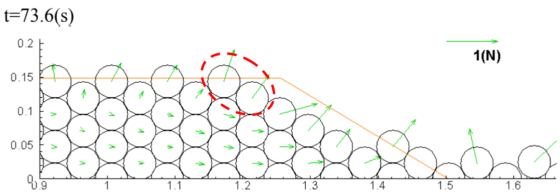

(b) Third stage destruction

Fig.8 Pressure distribution

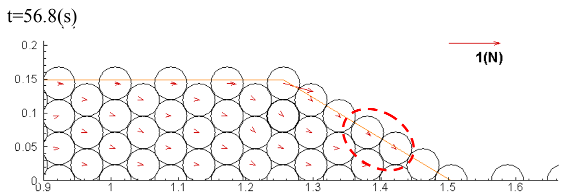

(a) Second stage destruction

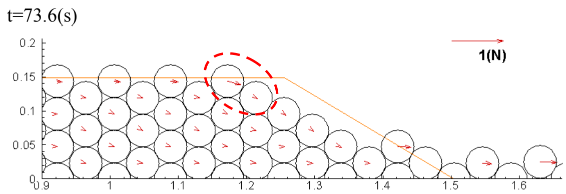

(b) Third stage destruction

Fig.9 Drag force distribution

14(l/s). Therefore, initial discharge for the numerical analysis was set at 10(l/s). Starting from the initial discharge, it was gradually increased in the analysis. No noticeable movement of the particles can be seen in the early stage of the calculation. Although the removal of the particle did not occur, particles start to vibrate when the discharge becomes larger than 15(l/s). In the experiment, initial destruction with the removal of loosely engaged stones on the downstream slope of the weir started when the discharge reached 14(l/s), whereas the numerical results did not show the removal of the particles. This result suggests that the particle engagement for the numerical analysis was not so loosely engaged as for the experiment.

Figure 6 shows the second stage destruction whose state was defined by Maeno et al.(2002). The required time was 56.8 s after the calculation started and the discharge at this stage was 17.1(l/s). First the particles located on the downstream slope of the weir started to move and were washed away. Second the particles located at the upper part of the washed particles fell there. After that, particles located around a shoulder part of the weir were washed away. This destruction process well describes the experimental results shown by Maeno et al.(2002). The velocity distribution in the Figure shows that the water invades the area where the particles are washed away. That is, the change of the flow with the change of the porosity can be also reproduced. This proves the validity of the porosity adjustment method proposed in this study. With respect to the discharge, a second stage destruction started when it reached about 17(l/s). In the experiment, the second stage destruction occurred when the discharge reached about 16.5(l/s). Numerical result agrees well with the experimental result.

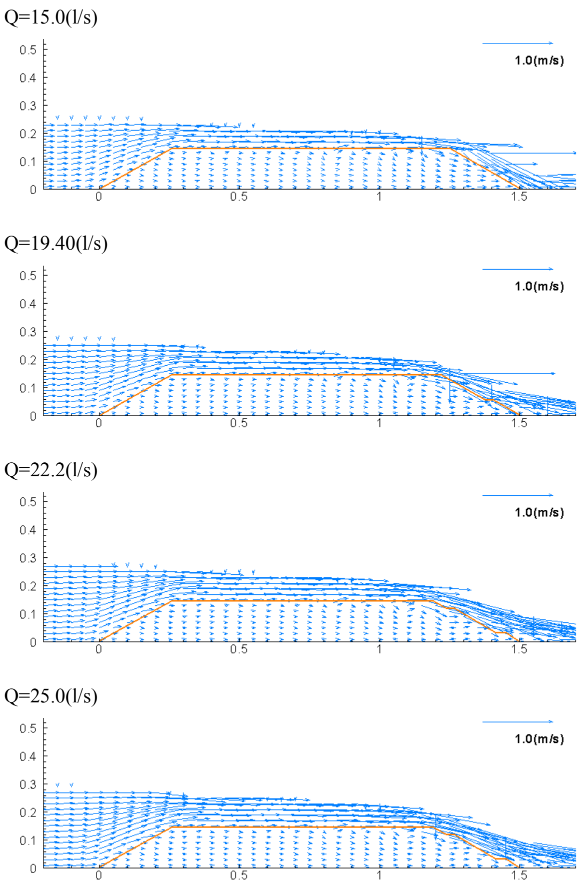

Fig.10 Velocity distribution in and around rubble mound weir

After the second stage destruction, although only one particle washed away, no noticeable destruction could be seen. In other words, a stable state was maintained for a while. With an increase of the discharge, 16 s after the second destruction, a third destruction occurred at a discharge of 19.2(l/s). **Figure 7** shows the third stage destruction. Unlike the second stage destruction, two particles located at the shoulder of the weir washed away. In the experiment the third stage destruction occurred when the discharge reached 20.4 (l/s). The proposed model can also reproduce the third stage destruction.

As mentioned above, the alternative destruction process of the rubble mound weir with destruction stage and the stable stage was well explained by the proposed numerical model. That is, the analytical model is effective as a failure prediction model of the rubble structure installed in the field.

3.2 Effect of pressure gradient and drag force

Figure 8 shows pressure gradient distribution when the second and the third destruction occurred. And the areas in a red broken line are the particles where they were going to move in right after. Maeno et al. clarified that the pressure gradient acting on the surface particles at the downstream slope plays an important role as for the removal of the particles there. With respect to the second stage destruction, as shown in Figure 8, a rather high pressure gradient was acting on the particles on the slope. The forces in the normal direction to the slope are acting on the particles on the slope. This result supports the tensile test results that the particles on the slope are easily moved to normal and vertical direction.

As for the third stage destruction, the same kind of upward forces occurred on the shoulder part of the weir. It was concluded that the pressure gradient had a large effect on the step by step destruction of the weir.

Figure 9 shows the drag force distribution caused by the flow around the particles. Although the drag forces increase near the shoulder region, its effect on the movement of the particles seems to be smaller compared with the effect of the pressure gradient.

3.3 Flow in and around the rubble mound weir

Figure 10 shows the velocity distribution in and around the weir with an increase of the discharge. First uniformly approaching flow turns the flow direction due to the existence the rubble mound weir. Although part of the flow infiltrates the rubble mound weir, most of the flow flows upwards along the upstream slope of the weir and flows onto the rubble mound. The flow velocity increases with flowing on the weir crown. The flow rate into the weir increases on the downstream side of the crown. The flow velocity and water depth gradually increase with an increase of the discharge. The orange line shows the outline of the weir. The progress of the weir destruction and the change of the flow distribution with an increase of the discharge were appropriately explained by the numerical analysis. Such features have been experimentally confirmed by Maeno et al. (2002), and it proves the validity of the numerical model.

4. CONCLUSIONS

In this study, the VOF-DEM coupled numerical model to simulate the flow and the destruction process of the rubble mound weir was proposed and its validity was investigated. Obtained main results are as follows.

1) Proposed VOF-DEM coupled model can reproduce not only the movement of the particles but also the flow region.
2) Destruction process of the rubble mound weir was properly explained such as the removal of particles on the downstream side slope of the weir and the collapse of the shoulder part of the weir with an increase of the discharge.
3) The step by step destruction of the rubble mound weir with an increase of the discharge were explained by the proposed numerical model.
4) Pressure gradient occurring at the downstream slope has a large effect on the movement of the particles there.

In this study, the effect of the initial packing and mixed particle size was not studied. Improvement of the accuracy of the model has to be done in a future study.

REFERENCES

Cundall. P. A. and Strack O.D.L. (1979), A discrete numerical model for granular assemblies, *Geotechnique* 29. No.1, pp.47-65.

Edward, C.C., Fue-Sang, L. and Yovanovich, M.M. (2000), Numerical study of forced flow in a back-step channel through porous layer, *34th, ASME Narional Heat Transfer Conference*, pp. 1-6.

Gotoh, H. and Sakai, T. (1997), Numerical simulation of sheet flow as granular materials, *Journal of Waterway Port Coastal and Ocean Eng*., *ASCE*, Vol.123, No.6, pp.329-336.

Gotoh, H., Harada, E. and Sakai, T. (2000) Movable-bed simulator for fractional transport of graded sediment, *Annual Journal of Hydraulic Engineering*, *JSCE*, Vol.44, pp.665-670. (in Japanese)

Maeno, S., Michioku, K., Morinaga, S. and Ohnishi, T. (2002), Hydraulic characteristics of a rubble mound weir and its failure process, *proc. of 5th ICHE Conference*, Theme D.(CD-ROM)

Maeno, S. and Michioku, K. (2004), Numerical simulation of the flow around a rubble mound weir, *4th International Symposium on Environmental Hydraulics*, pp.1809-1815.

Maeno, S., Michioku, K. and Kase, E. (2005), Failure prediction model of a rubble mound weir using distinct element method, , *XXXI IAHR Congress*, pp.3304-3311.

Maeno, S., Ogawa, M. and Bierawski, L.G. (2006), Modeling submerged breakwater using VOF-DEM-FEM, *Annual Journal of Coastal Engineering, JSCE*, pp.886-890. (in Japanese)

Maeno, S., Ogawa, M. and Michioku, K. (2007), E. Flow analysis passing a porous weir using vertical two dimensional model, *Doboku Gakkai Ronbunshuu B*, Vol.63, No.1, pp.16-28. (in Japanese)

Michioku, K., Meno, S., Haneda, M. and Furusawa, T. (2003), Analysis on discharge over and through a rubble mound weir, *Journal of Hydraulic, Coastal and Environmental Engineering*, *JSCE*, No.740, pp.131-142. (In Japanese)

Michioku, K. and Maeno, S. (2004), Study on Flow Structure and Discharge over a Permeable Rubble Mound Weir, Proc. *4th Int. Symp. on Environ. Hydraulics and 14th APD-IAHR*, pp. 1801-1808.

Michioku, K., Maeno, S., Furusawa, T. and Haneda M. (2005a), Discharge through a permeable rubble mound weir. *J. Hydraulic Engineering*, *ASCE*, Vol.131, No.1, pp. 1-10.

Michioku, K., Nanjo, M., Ishigaki, T. and Maeno, S. (2005b), Two-dimensional analysis on solid-liquid-phase flow in and open channel with a rubble mound groin, *XXXI IAHR Congress*, pp.2870-2879.

Michioku, K., Nanjo, M., Ishigaki, T. and Maeno, S. (2005c), A two-dimensional two-layer model for analyzing an open channel flow with submerged rubble mound groin, *Journal of Hydraulic, Coastal and Environmental Engineering*, *JSCE*, No.782/II-70, pp. 31-50.

Li Z., Michioku, K. and Maeno, S. (2007), Hydraulic characteristics of a group of permeable groins constructed in an open channel flow, *Proc. XXXII IAHR Congress*. (CD-ROM)

Hirt, C. W. & Nichols, B. D. [1981], "Volume of Fluid Method for the Dynamics of Free Boundaries," *J. Comp Phys.,* Vol. 39, 201-225.

Isobe, M., Yu, X., Uemura, K. & Takahashi, S. (1999), Study on development of numerical flume, *Proc. of Coastal Engineering, JSCE*, Vol. 46, No.1, 36-40. (in Japanese)

Isobe, M., Hanahara, Y., Yu, X. & Takahashi, S. (2001), A VOF-based numerical model for wave transformation in shallow water, *Proc. of International Workshop on Advanced Design of Maritime Structures in the 21st Century, PHRI, MLIT*, Yokosuka, Japan, 200-205.

Itoh, K., Higuchi, Y., Toue, T. & Katsui, H. (2002), "Numerical simulation of deformation of rubble structures by DEM and VOF," *Proc. of the 12th International Offshore and Polar Engineering Conference, ISOPE,* Kitakyushu, Japan, 714-721.